Building and Environment 148 (2019) 609–622

Contents lists available at ScienceDirect

Building and Environment

journal homepage: www.elsevier.com/locate/buildenv

Environmental response of a CLT floor panel: Lessons for moisture management and monitoring of mass timber buildings

Evan L. Schmidt[a], Mariapaola Riggio[a,*], Andre R. Barbosa[b], Ignace Mugabo[a,b]

[a] Dept. Wood Science and Engineering, Oregon State University, USA
[b] School of Civil and Construction Engineering, Oregon State University, USA

ARTICLE INFO

Keywords:
Cross-laminated timber
Mass timber
Moisture
Hygrothermal performance

ABSTRACT

Cross-laminated timber (CLT) is becoming increasingly adopted into North American construction, yet little is known about the impacts of environmental exposure (e.g., to rain during construction) on its long-term performance. The lack of protocols for on-site moisture protection in North America makes it a pressing matter to determine general moisture responses of this material in order to establish a behavioral baseline for practitioners and future researchers.

A CLT floor panel sample was exposed to cycles of wetting and drying in an environmental chamber. During these cycles, physical and geometrical properties of the panel were monitored. Testing results indicate that discontinuities in the layup CLT affects the hygroscopic behavior of the product. While the panel showed high dimensional stability, it also exhibited checking, cupping, and interfacial shearing after cycling. Bending test results before and after cycling indicated a reduction of the structural capacity due to the weathering.

1. Introduction

Wood has the capacity to serve as the primary structural material for mid-to high-rise buildings [1]. Before this is possible on a wide and standardized basis, research and design efforts must unite to verify the performance of so called “mass timber” building systems and the products that comprise them, such as cross-laminated timber (CLT). One performance category for buildings is durability, which in the case of wood can be strongly affected by prolonged exposure to moisture [2–4]. The absence of a standard protocol in North America for on-site moisture protection during transport and construction raises concerns regarding the relative wetting and drying ability of CLT, especially after enclosure within building assemblies. As a hygroscopic material, wood exchanges moisture with the surrounding environment. While wood typically resides in the 8–12% moisture content (MC) range in conditioned buildings, exposure to bulk liquid (e.g., a leak or rain during construction) or high relative humidity conditions (e.g., condensation build up in assemblies) can result in undesirable moisture gains well above the fiber saturation point (FSP, ~28%). MC changes in the hygroscopic range (typically 0–28%) affect nearly every physical and mechanical property of the material, and cause dimensional changes (i.e., shrinking and swelling) [2,3]. Importantly, mechano-sorptive effects in wood imply reduced stiffness and increased viscoelastic and plastic deformation with higher moisture contents [4]. When applied at the global scale, these changes (e.g., dimensional change with moisture change, creep, etc.) can impact building tolerances and result in settling [5,6]. Shrinkage and swelling could also have an effect on connection durability and stiffness [7].

Wood with a MC above the FSP is increasingly susceptible to fungal attack that ultimately reduces its structural integrity. Service conditions are thus stipulated that dictate the usage of wood products based on their anticipated equilibrium moisture content (EMC) after assembly and in service. Both the National Design Specification (NDS) for Wood Construction [8] and the APA North American Standard for Performance Rated CLT (PRG 320) [9] specify dry service conditions (< 16% MC) for CLT, unless otherwise specified by the manufacturer. The rate of moisture exchange between wood and the ambient environment is low, and surface moisture contents rarely exceed 20% in covered outdoor conditions [10], highlighting that the concern primarily lies with direct exposure to bulk liquid. Rapid moisture gains, especially followed by rapid moisture loss from a very dry interior climate, raise additional concerns related to the development of moisture induced stresses and strains (differential swelling and shrinkage) that can lead to checking, warping, and possibly delamination. Checking and delamination can potentially affect structural properties such as shear stiffness [11], and could affect other performance characteristics such as resistance to air, vapor and liquid flow. Rapid changes in moisture content have also been reported to affect connections capacity. Silva et al.

* Corresponding author. 236 Richardson Hall, Corvallis, 38131, OR, USA.
E-mail address: mariapaola.riggio@oregonstate.edu (M. Riggio).

https://doi.org/10.1016/j.buildenv.2018.11.038
Received 27 August 2018; Received in revised form 28 November 2018; Accepted 29 November 2018
Available online 30 November 2018
0360-1323/

[12] studied the influence of change in moisture content to the self-tapping screws (STS) withdrawal resistance in CLT samples. The study reported a 1.8% decrease in STS withdrawal resistance for each percent increase in CLT moisture content between 12% and 18% MC. Extensive studies have evaluated the effects of change in MC on the modulus of elasticity (MOE) and modulus of rupture (MOR) of clear wood and structural lumber [13,14], but few have focused on the impact of MC on the mechanical properties of CLT.

While there is a large body of literature on moisture transport in solid wood, there is less research on hygrothermal behavior of CLT, especially related to general implications of direct wetting. Hygrothermal studies on CLT have tended to focus on singular material properties for modeling—e.g., EMC or liquid diffusivity for suction and redistribution coefficients (A values) (e.g. Ref. [15])—and many face the difficulty of defining testing standards that captures the full-scale effects of the product particularly the effects of the matrix of gaps, checks, and general discontinuities on moisture ingress [15–18]. McClung et al. [19], Wang [20], Lepage et al. [21], Kordziel [22], and Schmidt et al. [23,24], conducted laboratory scale experiments emphasizing monitoring of wetting and drying behaviors of large CLT specimens. McClung et al. [19] found that 5-ply CLT specimens wetted by submersion for one week with epoxy-sealed edges and subsequently built into assemblies of varying permeability were generally within acceptable MC ranges (< 26%) after one month and were mostly dry after 4–6 months. They also observed that drying typically stopped after about 120 days. Conversely, Wang [20] observed that even six months of drying had only a small effect on the average moisture content of 3-ply epoxy edge-sealed CLT samples that had been wetted from above for two weeks and subsequently covered with an impermeable membrane above and closed-cell foam below. The data in Lepage [21] showed that edge-sealed CLT samples exposed to winter conditions registered high surface ply MCs that dried to below 15% in less than 6 months, and that cementitious toppings resulted in moisture trapping and high MC loads. Results in Kordziel [22] showed that absorption coefficients were 18–27% higher when CLT was wetted from above, rather than below. In addition, Kordziel monitored a CLT roof under construction and observed that impermeable roof membranes could strongly retard drying, with some locations remaining above 20% MC for over a year. Schmidt et al. [23] compared dimensional stability, checking, mass, and MC gradients of an edge sealed and non-edge-sealed CLT sample during wetting, finding that edges and gaps played a strong role in the general hygrothermal behavior. These studies [19–23] generally indicated that CLT is capable of drying to safe levels after a few weeks or less of wetting exposure, but is susceptible to long periods of moisture stagnation under certain moisture trapping conditions. The variety of conditions that affect hygrothermal performance (e.g., weather patterns, detailing and material quality) makes it critical to conduct additional tests to better understand moisture behavior of CLT. Since panel edges provide a unique condition (combination of end grain and tangential wood faces, with gaps and openings), and are not guaranteed to be protected during construction or in service, it is particularly important to understand their effect on the global moisture response of a CLT panel.

Another area of concern is moisture vulnerability at the center regions of the panel. While the core of CLT has demonstrated resistance to moisture gain when wetted through the faces [15,16,18,20,23,24] it has the potential to accumulate moisture under unfavorable conditions (as suggested by Wang [20], and demonstrated by analogous research on glue-laminated timber—GLT, and nail-laminated timber—NLT). Niklewski et al. [25] explored MC correlations between exposure and connection types in glulam members, finding that exposed end grain and moisture trapping conditions were conducive to prolonged MC problems. All of these factors again suggest that CLT could be uniquely vulnerable to moisture accumulation at water trapping connections, as well as at all four of its edges where end grain and large checks/gaps provide means for bulk ingress. Checks, gaps, and delamination—all expected to be exacerbated by weather cycling—are considered to play some role in the wetting and drying rates of the interior layers [15,16,19,20,23].

In order to address these various concerns, experiments were devised within the framework of a multiscale research project—SMART-CLT. The first phase of this testing program attempted to build on existing literature by exploring the general moisture response of a half-lapped Douglas-fir, CLT floor panel exposed to cycles of simulated outdoor weathering and indoor climate. These experiments were designed to observe and interpret general trends and vulnerabilities, as well as to develop strategies for protecting and monitoring mass timber structures. While inference is limited to one large panel as a sample, this experiment aimed to preliminarily assess CLT for: (1) the wetting and drying rates at a global scale, as well as at various depths and locations, (2) in- and out-of-plane dimensional stability, (3) checking and general physical deterioration associated with cycling, and (4) possible reduction in MOE and MOR. These behaviors are discussed in terms of applicable lessons and suggested protocols for moisture monitoring campaigns, including data interpretation and analysis, and practicable contributions to design and construction protocols.

2. Materials and methods

2.1. Sample and environmental chamber

A 5-ply CLT sample, measuring 213 cm in length by 203 cm in width by 17.1 cm thick, was manufactured from 3.5 cm × 14 cm Douglas-fir (*Pseudotsuga menziesii*) boards (V1 PRG 320 Grade Certification [9]) and melamine-formaldehyde (MF) resin (non-edge-glued). The sample was composed of two panels joined at the center by a half-lap joint with self-tapping screws (SDWS 22 × 6") with 15.2 cm spacing on center. Two edges of the sample were sealed with epoxy putty at large gaps, after which two full coats of marine grade epoxy resin were applied. This sealant—applied again during weathering to compensate for any minute cracking—was used to form a water and vapor tight seal on two edges, simulating non-edge conditions.

Prior to assembly, the sample halves were transported to the Green Building Materials Laboratory (GBML) at Oregon State University, where they remained for approximately 4.5 months at indoor conditions. The sample was then assembled and installed in the *Multi Chamber Modular Environmental Conditioning* (MCMEC) system (Fig. 1), which can moderate temperature (−30 to 40 °C), relative humidity (5–95%), water spray, and UV light.

Two overhead spray racks were installed at adjacent corners of the chamber (near the unsealed edges), with an arc of approximately 150°

Fig. 1. The DF CLT panel installed in the environmental chamber.

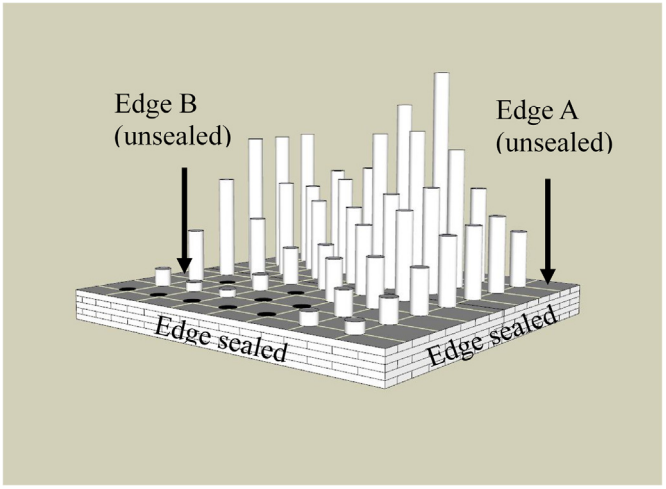

Fig. 2. The relative wetting distribution across the DF CLT panel. Wetting is concentrated towards the unsealed edges.

and an emitter pressure of 280 kPa. The relative distribution of wetting within the chamber was measured by placing 49 vessels on a square grid over the panel and calculating precipitation rate at each location, as indicated in Fig. 2.

The majority of water fell onto the front half of the panel and ran off in the direction of edge "B" (unsealed). Seven of the 49 vessels near the back were tipped over due to their proximity to the exhaust fan, but adjacent cups and a visual check confirmed that the entirety of the back panel was receiving precipitation.

2.2. Climatic conditions

Climatic conditions cycled between wetting and drying. Target ambient conditions (85% relative humidity– RH –and 9 °C) during wetting were averages chosen from weather data in Portland, OR, (November) [26] while precipitation rate (13.3 cm/week) was chosen based on the rainiest week in November since 2010 for the same location [26]. During wetting, spraying occurred in 2′53″ intervals every hour, for 15 consecutive hours per day. In total, there were three wetting cycles, the first lasting 11 days, the second 3 days, and the final 2 days.

Ambient conditions during controlled drying were set at 21/23 °C and 30% RH, generally coinciding with typical heated interior conditions during winter. The wetting and drying protocol intended to depict two scenarios. The first cycle simulated a fast construction schedule, with wet conditions during construction followed by in-service conditions. This could reflect a situation where a prefabricated enclosure is built after the erection of each floor. The scope of the following two cycles was to evaluate effects of repeated cycling, how they could occur in case of leaks during service or in some construction conditions (rainy days followed by sunny days). The last case is far from being unrealistic, as it has been confirmed by monitoring data in a building under construction [27]. Due to maintenance demands, the environmental chambers were shut off and opened during the latter half of the first drying cycle, leading to a slightly fluctuating climate (days 39–93) averaging 40% RH (standard deviation SD = 8.6%) and 24 °C (SD = 3.6 °C). Tertiary demands of complementary testing of the panel (and the need to stop chambers and open them twice weekly) produced abrupt (but brief) spikes in climate throughout the test. The objective of these tests was to observe behaviors during drying conditions, so these fluctuations should not specifically impact the results. Fig. 3 and Table 1 help to clarify the climatic conditions throughout the duration of the test.

2.3. Monitoring setup

Fig. 4 depicts the panel monitoring setup. The mass of the sample was measured using four load cells (Interface 2430 VLX – 8.90 kN capacity), which supported the panel from below on two opposite racks, including one that pivoted to allow for potential warpage. Voltages were read with a Hewlett Packard voltmeter (34740a, 34271b, 34701a), digitalized with a National Instruments shielded connector block (BNC-2110). The entire system was calibrated to within 0.45 kg. Voltages were read every 5 min at a sample rate of 5000 Hz for a total of two seconds (n = 10,000).

Additional measurements were taken twice-weekly while the MCMEC was off. Temperature fluctuations were corrected for using the manufacturer specification of 0.0036% increase in rated output per degree Celsius.

Moisture content was measured indirectly via the resistance method, which converts measured ohmic resistance values (from embedded electrodes) to moisture content values using manufacturer-dependent algorithms and corrections based on species and temperature. Both continuous and manual measurements were taken, with a listed uncertainty of ± 1% MC. Eight moisture sensors were installed for continuous measurements (manufacturer: Scanntronik MuGrauer; sensors: Gigamodul and Thermofox) at the bottom surface of the CLT panel. Three regions representing a gradient of exposure were chosen on the panel for these measurements, as shown in Fig. 4: "F" for front location, "M" for middle, and "R" for rear location.

MC probes at the "F" and "R" regions were installed at the center of plies 3, 4 and 5 (with ply 1 as the upper-most ply and ply 5 as the bottom-most). MC probes at the middle location were installed at the center of plies 3 and 4. Location and ply depth were demarcated, as an example, "M4", for the 4th ply at the mid location. The method followed for the installation of the probes was outlined by Dietsch et al. [28], though the embedded tips were not glued in. Silicone was applied to and around the external head of each sensor, as well as at the interface of the sensor with the wood to avoid corrosion, shorting of the sensors, and percolation of water along the interface. Hourly resistance readings were converted to MC and adjusted for species and temperature using Scanntronik's software. Thermistors were embedded at the center of both the second and third plies, which were inserted into bore holes and sealed with silicone.

In addition to continuous MC measurements, hand-held MC measurements (Delmhorst 18-ES resistance meter) were taken at the upper three plies (plies 1, 2 and 3) and from the top of the CLT panel. Measurements were taken: (1) six weeks prior to and one day after the first wetting, (2) one day after the second wetting, (3) one day before and one day after the third wetting. Measurements were taken one day after wetting cycles to allow for surface water to evaporate. Initially, handheld measurements were taken only near each continuous measurement region at the center of each ply due to concern over their semi-destructive nature. These holes were small, however, and could be sealed with silicone. Therefore, the third, fourth and fifth rounds of manual measurements were taken on a grid, with eight locations (Fig. 5) as well as a gradient of depths, starting at 1.3 cm below the surface, followed by approximately 0.6 cm increments until 8.1 cm total depth was reached. Measurements taken at different dates but at a "single" location (e.g. F2) were within a close proximity of one another, and with an attempt to keep distance to end grain consistent. For a single location it is assumed that the conditions were similar enough so as not to affect MC patterns as a result of distance to edges.

In addition to mass and moisture content measurements, dimensional and image-based data were collected on the sample approximately twice a week. Thickness measurements were made with digital calipers (± 0.01 mm resolution) on the two unsealed edges (edges A and B) with a measurement error of ± 0.05 mm. Edge A had eight evenly spaced locations for measurement, while Edge B had seven locations, three of which sat more tightly clustered in proximity to the

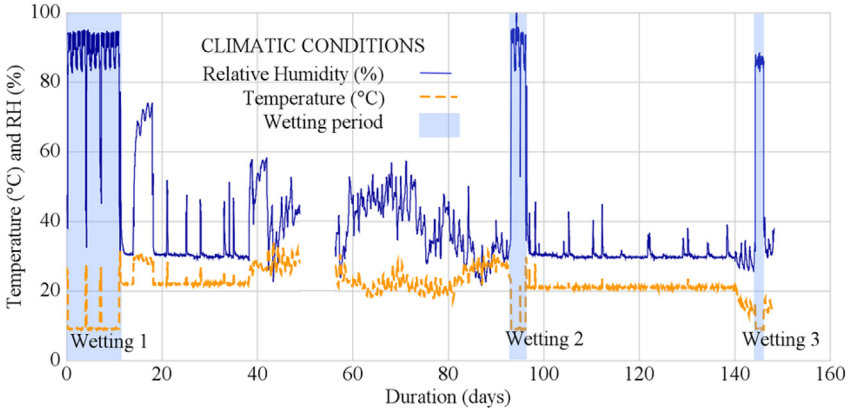

Fig. 3. Climatic conditions during testing.

Table 1
Statistics on ambient conditions during the various climatic cycles.

Cycle	Duration (days)	Mean % RH[a]	Mean temp.[a]
Wetting 1	11 days (0–11)	88% (9)	10 °C (3)
Drying 1	82 days (11–93)	39% (11)	24 °C (3)
Wetting 2	3 days (93–96)	90% (6)	9 °C (2)
Drying 2	48 days (96–144)	30% (3)	21 °C (2)
Wetting 3	2 days (144–146)	87% (2)	9 °C (0)

[a] Standard deviation in parenthesis.

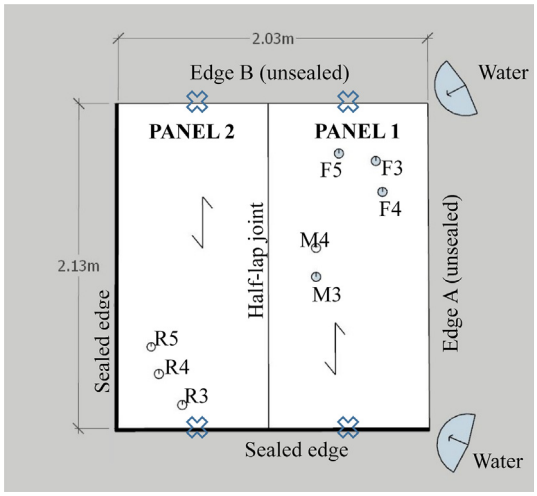

Fig. 4. A depiction of the panel installation and sensor layout. "X"s denote the location of the load cells. Directional arrows on the face of the CLT denote principle grain direction.

half-lap joint. In-plane dimensions were taken with a tape measure (roughly a 1.5 mm resolution). Images of the two exposed edges were collected using a photo-scanner (HP Scanjet, resolution 300 dpi) in order to document the evolution of checks and other discontinuities.

2.4. MOE and MOR characterization testing

Quasi-static three-point bending tests were conducted on the two individual CLT panels at two instants in time: (1) before the start of the moisture cycles, and (2) after the completion of the moisture cycles. Both tests were performed at 21.1 °C ambient temperature. Both sets of bending tests were conducted to measure the apparent MOE, according to ASTM D4761 [29], and the estimated CLT MOE values obtained at both instants in time were compared to discern any quantifiable changes in apparent MOE. During the post-moisture cycles bending

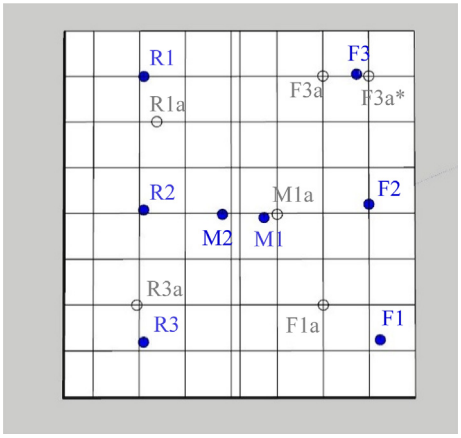

Fig. 5. A depiction of the locations of discontinuous moisture measurements. Empty circles are original locations, dark circles are adjusted locations. Each square on the grid is approximately 27 cm wide and long.

tests, the two CLT panels were loaded to failure to estimate the peak load and compare the MOR values to those obtained in a similar testing featuring similarly short span-to-depth ratios [30]. Results used for comparison are 22 DF CLT short span-to-depth bending tests that were performed to failure under flat-wise three-point loading.

The flat-wise three-point bending tests were conducted using a 1459 kN actuator with a 50.8 cm stroke. The panels were supported in a simply supported configuration allowing a 203 cm clear span, l, and 5.1 cm overhang on both sides of the panels. The resulting span-to depth ratio is 11.6. Fig. 6 shows photos of (i) the overall bending test setup, (ii) the deflection-measuring device, and (iii) a panel support location. The panels were continuously supported along the width, b, at the supports. A linear variable differential transformer (LVDT) transducer measures the center-point deflections, Δ, along the mid-height of the panel and at the mid-span. A 5.1 cm wide steel beam was placed under the loading cell and was used to spread the center-point load along the width of the panels. The panels were loaded within their linear elastic ranges up to approximately 10% of the predicted failure loads to mitigate bending test-induced panel damage.

$$E_{app} = \frac{Pl^3}{4bd^3\Delta} \quad (1)$$

where P/Δ is taken as the slope of the load-deflection diagram in the linear elastic range of the loading response, l is the panel's clear span, b is the panel's width, and d is the panel's depth.

After completion of the MC cycles, the panels were loaded up to failure. Using the peak loads, the MOR, S_R, for the individual panels were computed using:

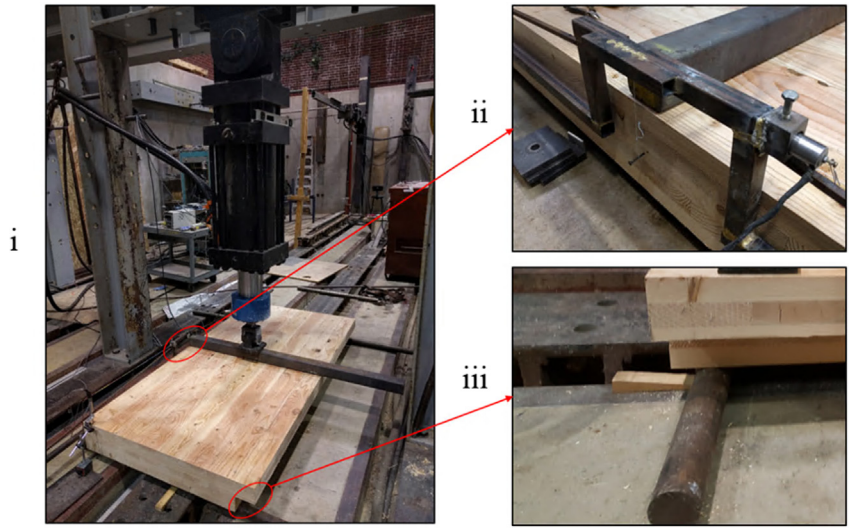

Fig. 6. Flat-wise center-point bending test photos: (i) overall bending test representation with the LVDT location circled around, (ii) close-up of the center-point LVDT transducer, (iii) close-up of a support location.

$$S_R = \frac{3P^l_{\max}}{2bd^2} \quad (2)$$

where $P_{\max}$ is the peak load prior to failure, l is the clear span of the panel, d is the panel's width, and d is the panel's depth.

3. Results and discussion

3.1. Data post processing and error analysis

Literature provides estimates of measurement uncertainty for resistance-based moisture content due the biological variability within a given wood species and at different moisture contents (e.g. Refs. [31,32]). In this study, both continuous and discontinuous readings were corrected for Douglas fir considering the manufacturer's calibration for this species. The manufacturer's calibration was not verified by comparison against oven-dry tests.

Data collected during weathering suggested that localized MC fluctuations were sometimes clearly correlated with external conditions, while at others they were of unclear origin. A review of the literature highlights the fact that issues with resistance based moisture content sensors—are ubiquitous, particularly when sensors are placed in highly fluctuating environments [2,22,25,33–36]. Resistance-based MC measurements are particularly sensitive to environmental interference due to the increasingly low amperes (e.g., 1×10^{-12} A) they measure with diminishing MC [36]. The factors most identified as having potential impacts on MC readings are: electromagnetic interference from neighboring devices (e.g. computers, generators, compressors) [2,26,36]; checks/gaps forming in the wood between electrodes and/or loss of contact with the wood substrate at the tips [2,25]; poor temperature correlation for correction [2]; and condensation on/or corrosion of the sensors [25,28–34,36]. The majority of literature does not deeply discuss irregularity in readings and the data are generally presented raw. In a few cases, post processing techniques were discussed and included the use of moving averages [2,25]. Niklewski et al. [25] post-processed their data by omitting segments of data considered unreliable based on a relative fit to a moving average. They also screened data, and removed larger periods of unreliable readings, or entire sensors if they were deemed "too erroneous." Removal of some data could be justified using other parameters, such as the reliable moisture content reading range of a sensor (e.g., standard between 5 and 25% for resistance readings), or a fit to a hygrothermal model. In terms of temperature, Gamper et al. [2] thoroughly reviewed the subject of correlations and error. Their data indicate that even precise location of sensors, or the use of values from heat transfer modeling (Euler method), while highly effective, still had some dissonance when dealing with large temperature ranges.

In order to clarify the cause and the potential magnitude of disturbances observed in the data from the weathering cycles, additional tests in the MCMEC on fully equilibrated and sealed CLT samples were conducted, with the aim of isolating certain environmental parameters suspected to influence readings (electromagnetism, temperature and condensation) [27]. In particular, this study investigated the unaccounted-for step-change increase in MC readings observed in every sensor during the exact duration of each wetting cycle (average increase of 0.56% MC; SD = 0.13%; first two wettings), which was indicative of a bias in the correction, or a faulty correlation between the temperature at the thermistors and the MC probes. These additional tests, which in part isolated the effects of temperature on MC readings in equilibrated samples, showed correction overcompensations of very similar magnitudes observed during the primary weathering experiment. This slight over-correction was corrected for by calculating the average increase in registered MC at the interface between the drying and wetting cycles for each sensor, and then subtracting them from the duration of the wetting cycle measurements (similar to a seasonal correction in a time series). There was good correlation between the resultant corrected plots and the raw MC measurements taken during the wetting cycles while the chamber was open, off, and at room temperature (at similar temperatures to the drying cycle), providing further evidence of method validity. For visual reference, Figs. 8–10 provide both raw data as well as corrected data using the post-processing method described above.

Other post-processing adjustments primarily included the removal of erroneous data. Since the manufacturer lists the threshold MC value of 5% as the lower boundary of reliable MC values, any values below this threshold were automatically removed. These were generally only erratic singular measurements, or, as seen in R5 (Fig. 10), what appeared to be occasional loss of contact between the probes and the wood. Sensors at F3 and R3 experienced persistent erratic readings following the onset of drying and were manually omitted, even though the first portion of F3 was retained, however. Niklewski et al. [25] described similar issues with readings (e.g., step changes and lost contact) and attributed them to internal checking and loss of contact between the electrodes and the wood. Finally, every sensor experienced a mild to moderate disturbance in readings after the first drying cycle began, which consisted of an unrealistic drop in MC, lasting approximately 10 days. It is difficult to clearly attribute a cause to this, but it

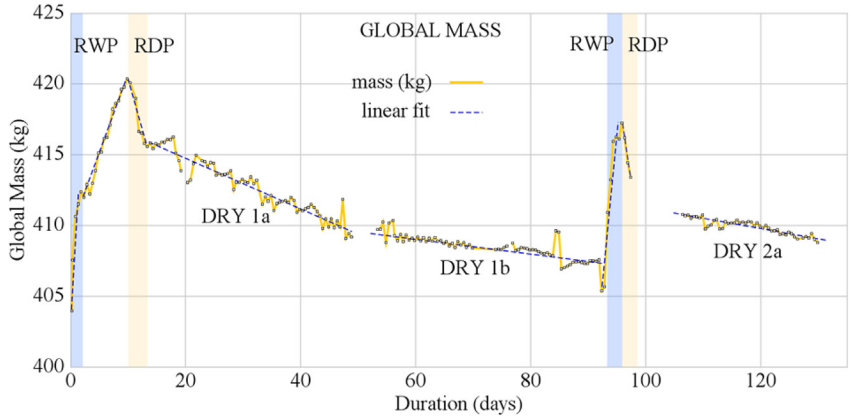

Fig. 7. Global mass of CLT sample plotted on a 12 h basis. RWP = rapid wetting period (blue shading). RDP = rapid drying period (yellow shading). (For interpretation of the references to colour in this figure legend, the reader is referred to the Web version of this article.)

could be a combination of erratic temperature correlation (exacerbated by complex MC distributions), internal checking, and/or condensation on the pins internally (if gaps were opened nearby and vapor was driven into them). Again, these values were included in the plots for reference, but were omitted from the 48-h moving averages (Figs. 8–10).

3.2. Global mass

Fig. 7 shows the global moisture content (GMC) change (measured by mass) during the weathering cycles. A maximum GMC increase of approximately 4.5% (16.1 kg added water mass) can be observed after 11 days of wetting (cycle 1). This value became roughly 3.5% (12.6 kg over 11 days wetting) when excluding what we will refer to as the "rapid initial drying phase"— RDP— (approximately the first 2 days of drying, which removes surface water). The second wetting cycle showed similar levels of gain (when excluding RDP, 3 kg of retained gain over 3 days of wetting). These values assumed an average starting moisture content of 12% in the panel and a consequent panel dry weight of 360 kg. Note that a 2% change in assumed average starting MC has an impact of less than 0.1% on the GMC calculations (i.e., 4.5% and 3.5% ± 0.1%). These figures are particularly interesting, considering [20]—in which samples were wetted in a similar manner for 14 days—observed an increase in GMC of 13% (from an average of 12%–25%) in edge-sealed CLT samples. The lower amount of global absorption observed could be due to a combination of the slightly shorter duration of wetting, thickness of the samples, species dependent resistance to diffusion and capillarity via pit aspiration [4], or other environmental factors such as precipitation volume, distribution and drainage slope.

A high initial rate of mass change, was observable during both the wetting and drying phases—a consequence of both pooling/evaporating surface water as well as the buffering effect of wood against MC change with increasing depth (e.g. Refs. [3,4,37]). The first 2–3 days of wetting during the first two cycles showed the most rapid rates of moisture gain, approaching +1% GMC/day (average + 3.4 kg/day, SD = 0.1 kg, n = 2; based on a linear fit, Fig. 7). After this, wetting slowed to approximately +0.3% GMC/day (1.1 kg/day, n = 1; first cycle). The panel lost moisture at a rate of approximately −0.6% GMC/day (average −2.31 kg/day, SD = 0.51 kg, n = 2) during the RDP. Subsequent drying rates were much slower, however, during the following 36 days (1st half of dry cycle 1; −0.05% GMC/day; −0.18 kg/day) and the 44 days after that (2nd half of dry cycle 1; −0.02% GMC/day; −0.06 kg/day). Drying during the second cycle appeared to be somewhat slower, starting out at −0.02% GMC/day (−0.05 kg/day) after the RDP. Overall, these values confirm McClung's observation [19] that most of the drying occurs in the first month after wetting (about 60% of total moisture retained after RDP was lost within the first 36 days of drying).

The sample took approximately 10–12 days of drying for every day of wetting exposure to approach near original MC values, though it never fully dried. The rate of mass-loss dropped to below −0.02% per day during the latter half of the first drying cycle, as well as the entirety of the second drying cycle, moisture was trapped in the more inert interior zones of the panel. The observation of higher core MCs is supported by results in McClung et al. [19], whose data showed slightly increased moisture contents (1–2%) at the core of many of the CLT specimens, even after a year of drying.

Expressing the water uptake on an area basis, it results that the panel absorbed 2.9 kg/m^2 after the first wetting cycle. This result is comparable with the range (1.8–3.2 kg/m^2) measured by Kordziel [22] after 10 days (top-side wetting). The higher core MCs indicate that while moisture was slow to enter the interior of the panel, it also lingered there during the entirety of the drying season. This moisture accrued at the center, even though these studies involved only a single wetting event lasting two weeks or less. The tendency for water to diffuse towards the interior of the panel, even during exterior drying conditions, was also inferred by continuous MC measurements that showed a lag in peak MC values at more interior locations long after drying began (Figs. 8 and 9). The potential for moisture to incrementally accrue at the interior of a panel has important implications for construction conditions, particularly in climates where frequent rain events are accompanied by long bouts of high relative humidity that restrict evaporative loss.

3.3. Moisture content measurements: areas most and least prone to wetting

Figs. 8–10 show plots of continuous measurements at the bottom three plies for locations depicted in Fig. 4. Fig. 11 shows post- and pre-wetting MC gradients in the three uppermost layers measured through discontinuous readings with the handheld resistance meter. The discontinuous measurements are averages of readings in the front, mid, and rear regions (Fig. 5), respectively. The data refer to the last two wetting events and the last drying event. The complete series of measurements is available in the appendix. Continuous measurements showed relatively small MC increases (+2% MC or less), while discontinuous measurements showed higher MC gains. The discontinuous measurements also highlighted the tendency for moisture to concentrate at the interface of the two uppermost plies following wetting events, rather than at just the uppermost surface. A recent study by Morrell et al. [38], which used CAT scans to observe MC concentrations in exposed CLT, also displayed this tendency. The mid location (at the half-lap joint) showed higher MC concentrations at each of its measured interfaces after wetting. While all of the interfaces also showed rapid

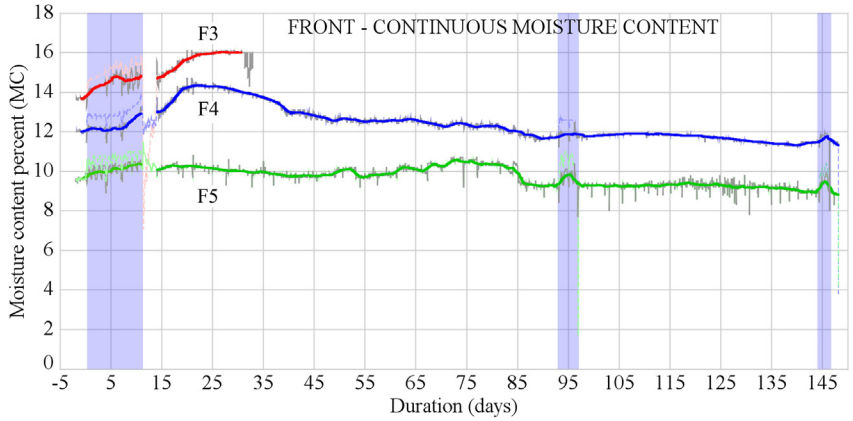

Fig. 8. Continuous moisture measurements at the front location. The thick lines are 48-h moving averages. The thinner lines are original data. The shaded areas are wetting periods.

drying, moisture accumulated in the interior of the 2nd and 3rd plies near the half-lap.

The tendency for moisture to accumulate at the interface of the upper two plies is due to the gaps between boards on the surface (non-edge-glued plies), which allowed liquid to both pool as well as physically bypass the first ply directly into the second. These gaps averaged 3 mm wide and appeared to, at times, interface with other gaps and air pockets below (e.g., the gaps between the ply 2 boards below, wane, and loose knots), providing direct routes into the interior of the panel. Fig. 12 (i) shows a surface gap (day 140, prior to wetting cycle 3), in which a large wane pocket is visible in the ply below, serving as an example of the potential for a matrix of openings, which evolve over time. Note the visible cracks in the resin at the large gap at the interface with the sub-ply. Fig. 12 (ii) is the upper half-lap after disassembly of the sample (day 150, after wetting cycle 3), illustrating the same wane pocket alongside others in the 2nd ply, all showing moisture concentration around the wane. The accumulation in both the 2nd and 3rd ply interfaces at the half-lap appears to be the result of moisture accumulating around the gaps and wane.

Continuous measurements at R4 and R5 (Fig. 10) displayed a general trend of moisture content decrease (approximately 1.5% MC loss over the entire measurement period), during drying. R4 lost moisture at similar rates as R5, indicating that the gaps in the bottom surface ply may have facilitated more rapid drying at the second layer, similar to how discontinuous measurements showed that areas near gaps appeared to wet as well as dry faster. F5 showed only small changes in MC, despite similar conditions to F3 and F4 (the two plies directly above), which showed MC increases of circa 2% (Fig. 8). Moisture may have had better access to diffuse into the wood tangentially near sensors F3 and F4 as a result of the gaps between boards that served as conduits into the panel. The lowest board, F5, however, had gaps that drained (with no ply below to hold water) and a higher exposed surface area, potentially resulting in these lower MC measurements.

3.4. Moisture retention and connections

Discontinuous measurements 15 cm away from the half-lap connection (Fig. 11 “MID” and Table 4 in the appendix) showed high moisture gain and retention in the 2nd and 3rd plies, even during extended drying (130 days of cumulative drying, with just 14 days of cumulative wetting). Continuous measurements at the mid location (M-3 and M-4), about 30 cm away from the half-lap, did not show this trend as clearly, although they showed slightly lower drying ability than the front and rear locations. Moisture levels observed near the half-lap could reasonably account for the higher global panel mass observed after drying. Moisture retention was anticipated at this joint, since the presence of channels with little air flow are prone to moisture trapping and are particularly vulnerable when coupled with unsealed end grain [3,25]. Since moisture appeared to fluctuate and/or accrue primarily at edges, gaps, and connection conditions, it follows that these locations present the greatest concerns regarding moisture ingress and its affiliated issues (e.g., checking, dimensional stability, etc.). This risk is critical since connections play a primary role in defining the stiffness and dynamic characteristics of timber structures [39].

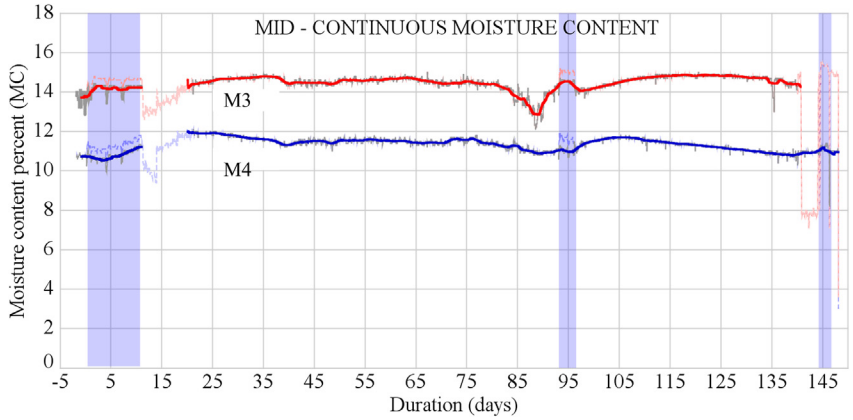

Fig. 9. Continuous moisture measurements at the mid location. The thick lines are 48-h moving averages. The thinner lines are original data. The shaded areas are wetting periods.

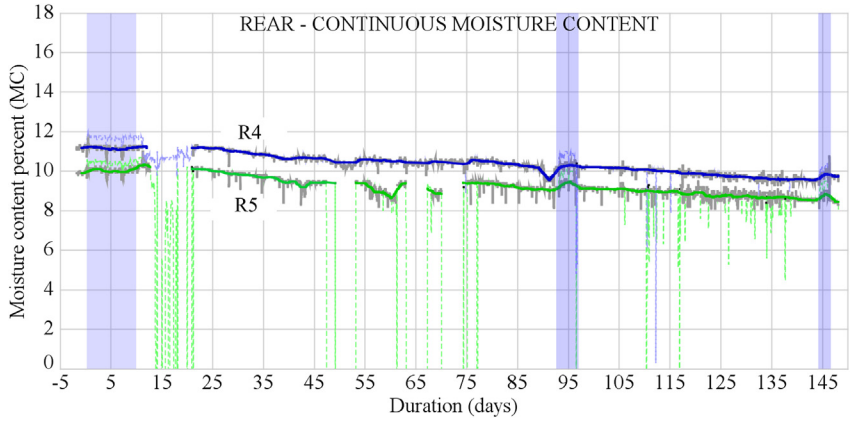

Fig. 10. Continuous moisture measurements at the rear location. The thick lines are 48-h moving averages. The thinner lines are original data. The shaded areas are wetting periods.

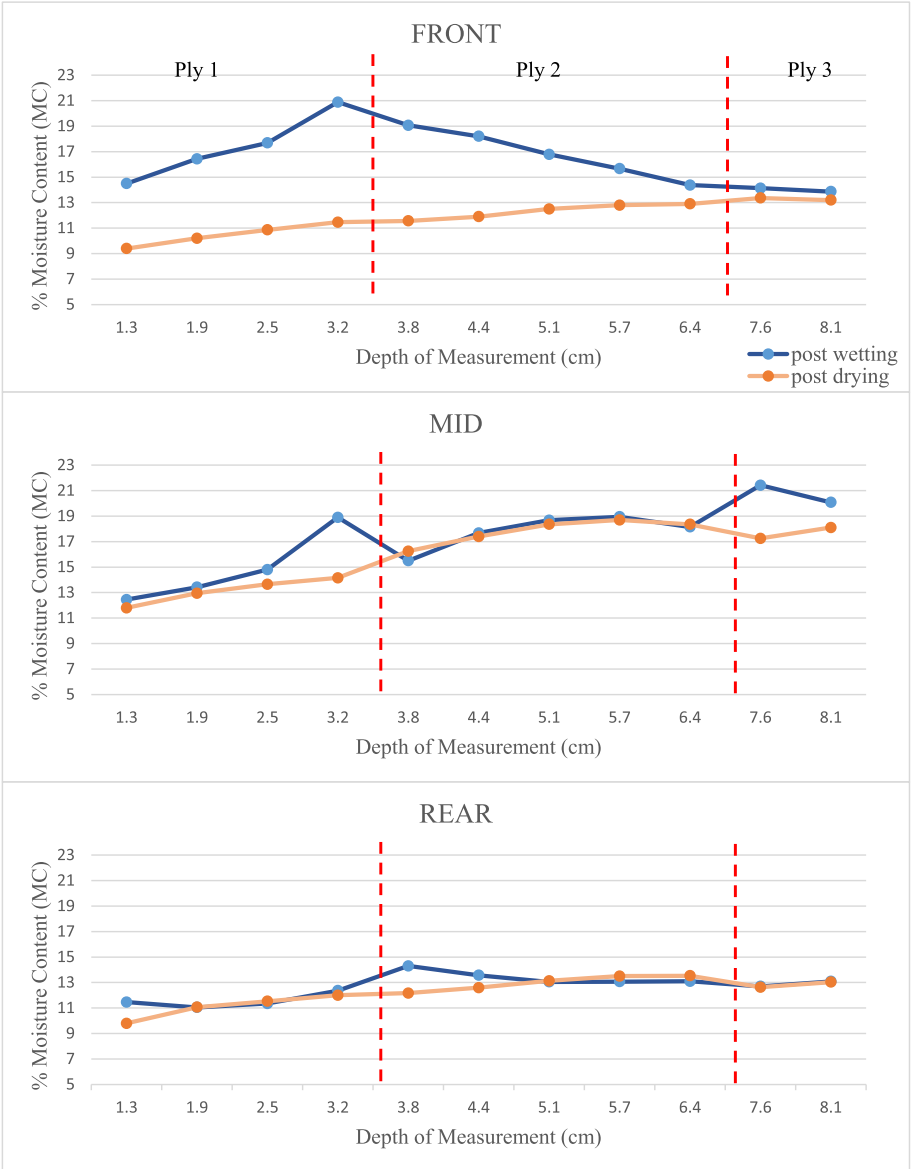

Fig. 11. Average values of proximate, discontinuous moisture measurements in the three uppermost plies at the front, mid and rear location, after wetting and after drying.

Fig. 12. Wane in the CLT panel. (i) — Wane clearly visibly through surface gap. Note cracks in resin. (ii) — Wane visible in the second ply after disassembly of the half-lap joint.

3.5. Dimensional stability and physical deterioration

Due to the restraining action of the cross laminations, CLT has (relative to uniaxial laminated timber products) stable in-plane dimensions as it fluctuates with the environment. The sample expanded a maximum of 0.16% (31.8 mm) in width (measured transverse to the surface plies in-plane) and 0.04% (7.9 mm) in length (measured longitudinally in-plane) during wetting. These displacements were still markedly smaller than standard unrestrained rates for the used wooden species. For example, a 0.04% longitudinal increase in Douglas-fir should typically correspond to about a 10% increase in MC, which would produce about a 2% increase in transverse (across grain) dimensions [3,41]. Out-of-plane (thickness) dimensions fluctuated at relatively typical unrestrained transverse rates. Edge “B” and edge “A” swelled by a maximum of approximately 3.5% (6.2 mm) and 2.0% (3.6 mm), respectively (Fig. 13), which correspond to a 10–15% average MC increase near measurement locations. The discrepancy between the two thickness values is reasonable, because edge “B” had three lamellas with exposed end grain (as opposed to edge “A” which had two), was the edge towards which water drained, and had more checking and gaps for potential bulk liquid entry.

The in-plane dimensional stability of CLT, while beneficial, comes at the cost of engendering perpendicular-to-grain tensile stresses with moisture change, particularly at the interfaces of the plies and at the edges. These inter-laminar stresses are developed by constraining moisture-induced transverse swelling and shrinkage by the adjacent longitudinal lamellae and are—if large enough—relieved by physical deterioration (e.g., cupping, checking, interfacial shearing, and possibly delamination, where delamination is defined by bond-line failure, and interfacial shearing is defined as wood failure along the bond-line [40]). In addition to these inter-laminar stress gradients, wetting and drying of a panel alternatingly induces tensile stresses at both the shell and core of the panel itself [41]. In other words, CLT has a dual-restraint effect: 1) an *inner-outer* restraint, where the core and shell restrain one-another, and 2) an *in-between* restraint, in which each lamella laterally restrains its neighbors. The resultant restraint-induced checking can, in theory, occur at all depths and multiply/deepen over time, which is what is referred to as the “zipper effect” [2]. Ambient indoor humidity fluctuations can exacerbate these discontinuities, but this deterioration is primarily pronounced by extreme fluctuations, e.g., wetting during construction and the first drying season after installation [2]. Since this deterioration produces an increasingly open and discontinuous panel for liquid and vapor to enter, there is a chance that panels might become increasingly vulnerable to environmental exposure the longer they have been exposed [23].

The effects of physical deterioration were observable in thickness measurements (Fig. 13), which indicated a displacement from original dimensions with cycling. Edge “B” showed greater displacement than “A”, as well as greater levels cycling-induced damage. Interfacial shearing was pronounced at the gaps between boards at the interface of the exterior plies (1 → 2; 4 → 5), where large MC fluctuations resulted in cupping (Figs. 14 and 15).

3.6. MOE and MOR characterization testing

For reference, the MC of the individual specimens were measured with a capacitance moisture meter before the pre-moisture cycle and post-moisture cycle short-span bending tests. At the time of the pre-moisture cycle tests, Panel 1 and 2 weighted 208 kg and 206 kg, respectively, and MC readings averaged at 14% MC for each of the two

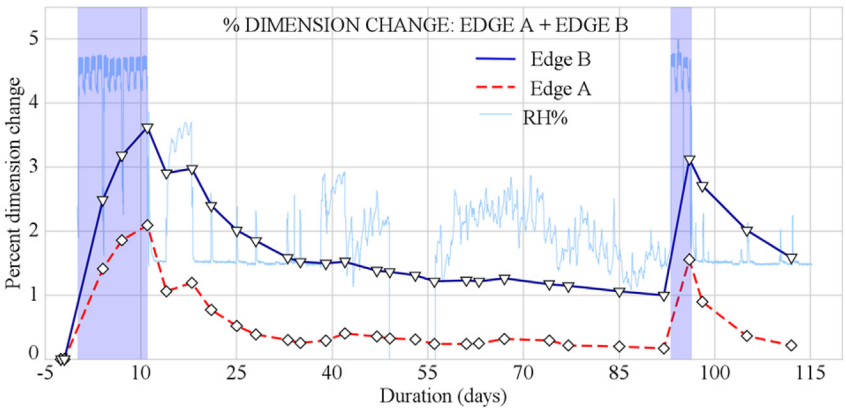

Fig. 13. Percent dimension change in the thickness of the panel at its edges A and B.

Fig. 14. Edge B before and after weathering. (ii): Edge B after two cycles of weathering. (i): edge B before weathering.

Fig. 15. Checking, cupping, and general deterioration of the panel observed in edge B near the half-lap joint after weathering.

panels. After the completion of the moisture cycles, the panels equilibrated to indoor conditions. Before the post-moisture cycles short-span bending tests, the panels' MC averaged at around 10%. Panels 1 and 2 weighted 197 kg and 196 kg, respectively.

Table 2 presents the apparent MOE values before and after the introduction of the moisture cycles. Panel 1 exhibited approximately 10% reduction in apparent MOE, while panel 2 exhibited a 4% increase in MOE. Panel 1 experienced more extreme moisture cycles compared to panel 2, due to the positions of the water sprays in the MCMEC chamber. This experimental setup condition could explain the observation of panel 1 displaying a notable reduction in apparent MOE. Considering that both panels had a lower MC when tested in the post-moisture cycles bending tests (4% lower), the increase in MOE in panel 1 could be attributed to the reported increase in lumber structural properties as moisture contents decrease [13,14].

In the post-moisture cycles bending tests, the CLT panels were tested to failure. The two panels failed under rolling shear of the transversally loaded plies. Fig. 16 presents examples of locations where the rolling shear failure mechanism was observed. The rolling shear failure mechanism was also determined to be the main mode of failure for the short-span CLT panels tests reported in Mahdavifar [30]. The mean MOR of the 22 short-span CLT panels in Mahdavifar [30] was 32.41 MPa, with a coefficient of variation of 8.20%. The MOR, S_R, of the panels A and B are presented in Table 5. The MOR of panel 1 and 2 were equivalent to 83% and 69% of the mean MOR estimated from the short-span bending tests in Mahdavifar [30]. The lower MOR values of the weathered panels indicate that strength properties of the panels were negatively affected by their exposure to the moisture cycles regime.

Table 2
Apparent MOE and MOR values of panel 1 and 2.

	Pre-MCR E_{app} [GPa][a]	Post-MCR E_{app} [GPa][b]	S_R [MPa]
Panel 1	8.93	8.13	27.00
Panel 2	9.38	9.79	22.27

[a] Pre-MCR stands for Pre-moisture cycle regime.
[b] Post-MCR stands for Post-moisture cycle regime.

4. Concluding remarks and recommendations

Due to the limited research on full-scale moisture performance of CLT, as well as the lack of standards in the US stipulating protection of mass timber elements during construction, a research need was identified to define a base level of performance to guide local industry. In particular, it was deemed necessary to develop a deeper understanding of the general hygrothermal response, to elicit strategies for moisture management and improved manufacturing/design procedures, and to refine moisture monitoring protocols.

4.1. Summary of hygrothermal findings

The most vulnerable areas of the exposed CLT floor panel were the two upper layers, in particular at the interface between the two upper plies, and anywhere near the end grain, gaps and the half-lap connection. The half lap joint was particularly vulnerable, showing substantial moisture retention at the center plies during extended drying. Global mass measurements also reflected moisture retention. CLT dries at a slower rate than it wets because of 1) the high speed with which moisture concentrations develops via exposure to bulk liquid, versus bound water and vapor diffusion, 2) the effects of sorption hysteresis (desorption to higher MCs than adsorption), and, 3) the tendency of accumulated moisture to diffuse in all drier directions in wood (even towards the interior), despite external conditions themselves being conducive to drying. For this reason, the core layers, while mostly inert to rapid ingress, appear capable of accumulating moisture with repeat wettings, and of storing that moisture for longer periods of time. This, along with high MCs registered at the center of the panel near the joint, show that surface measurements taken during construction are not necessarily a good indicator that CLT is ready for enclosure within a non-permeable assembly.

Exposed end grain was primarily an issue where it was coupled with moisture trapping conditions (e.g., the half-lap) and it appears that repeat wettings could lead to small but incremental accumulation of moisture at the interior of the panel. Areas near exposed end grain dried relatively quickly once wetted, but the issue remains that large MC fluctuations can have degradative effects on the panel. Since the edges of the panel are highly susceptible to rapid moisture ingress and loss, they (like the various gaps and interstices) are subsequently more prone to moisture related damage.

Based on the testing results, rapid fluctuations in moisture content appear to have a negative impact primarily on the MOR. The MOR of low span-to-depth ratio panels is mainly governed by rolling shear failure. The apparent MOE of short-span CLT panels appears to be less impacted by the moisture fluctuations in comparison to the MOR.

4.2. Limitations and future research

The conclusions of this study are limited to the general behavior of a single CLT floor sample and do not reflect the potential intra-and inter-manufacturers variability. Species, board size, board grade, press type, resin, edge-gluing, MC at layup, equilibration history, and sealants are all examples of manufacturing parameters that will have varying effects on hygrothermal performance. These intrinsic quality differences are compounded by extrinsic ones, e.g., the change in the characteristics of

Fig. 16. Rolling shear failure mechanism. The red oval shapes shows rolling shear failure locations. (For interpretation of the references to colour in this figure legend, the reader is referred to the Web version of this article.)

the material as it evolves over time with exposure. For modeling purposes, more rigorous hygrothermal tests are needed that account for the variability, realistic exposure angles, and scale of CLT. More date are needed on the rate of sorption and redistribution when wetting the faces of CLT from above in addition to from below (as in Ref. [22]). Moreover, there is a need to further establish: 1) a base range of variability of anticipated hygrothermal performance during and after construction, 2) the linkage between gaps and wetting/drying potential, and 3) the effects of more realistic and prolonged wetting exposures, since outdoor exposure will embody longer exposure periods and more frequent and diverse weathering cycles (e.g., from daily temperature swings, freezing and thawing, etc.). Limited structural testing was performed, however a trend in reduction of the structural capacity due to the weathering was clearly observed. Future study should include statistically significant samples to quantify the effects of damage due to weathering cycles in the engineering design values.

4.3. Lessons for moisture monitoring

Resistance based moisture measurements are sensitive to environmental conditions and care must be taken during installation to limit possible interfering factors. The issues that seem most difficult to avoid, depending on the study, are:

(1) Internal checking of the panel or loss of contact with the wood as a result of heavy environmental flux. Gluing the probes in place, as suggested by Dietsch et al. [28], may help with the latter. The presence of internal gaps also indicates the potential for development of condensation on the probes within the panel. These issues might manifest as temporary or permanent sudden shifts in measured MC with environmental flux. Sensors in the center of the panel might be more prone to such disturbance, as mentioned by Niklewski [25] and observed in two out of the three installed 3rd-ply probes.
(2) Sensitivity and bias in correlations between temperature sensors and the MC probes. Even with thermistors embedded at representative layers, large temperature swings and variability in locations might produce some irregularity in readings. An average overcompensation of approximately 0.56% MC was observed with temperature drops of 16 °C. These errors will generally be minor, so long as the thermistors are placed in such a way as to reflect similar conditions as the MC probes.

Moisture distribution was observed to vary substantially even in close locations, due to the non-homogeneity of wood and the complex geometries of CLT (also supported by Ref. [38]). A larger number of permanent sensors would be ideal to more richly assess moisture distribution trends, such as at the center of plies and adjacent to gaps or other lamella. In general, the limitations of continuous resistance sensors includes the potential for corruption and a limited representation of complex MC distributions in a sample. Handheld measurements proved an invaluable addition for collecting such rich data at a given location in time, but were semi-destructive, time intensive, and required continuing access to the panel.

4.4. Suggestions for manufacturing, design, and construction

Improving the performance of CLT will involve developing moisture-related standards in manufacturing, design and construction, with the associated costs of these preventative measures weighed against the potential costs of remedial action. The single most effective measure would be to prevent direct liquid intrusion into the panel by physically sheltering it, or at the very least covering or sealing all vulnerable regions, e.g. end grain, connections and cutouts. On the manufacturing side, a few ways to achieve better performance regarding intrusion might include: (1) utilizing higher grade lumber that has less wane, loose knots, and other potential channels/reservoirs, (2) laying-up boards at a MC that is closer to, or below, their anticipated service EMC, so that they do not excessively shrink prior to, during, or after installation. Edge gluing would likely provide increased resistance to liquid entry during construction, but will inevitably crack again during drying [42].

In general, buildings will be most vulnerable at areas of complex detailing, particularly at connections, edges and cutouts (balconies, corners, windows, doors, service openings, hardware routes, skylights and flashing, etc.). The simplest construction measure, although perhaps not the cheapest, would again be to keep the panels themselves physically protected from rain. This might be achievable by emphasis on prefabrication, rapid construction and clever phasing, or it might simply involve using a canopy structure where possible (e.g. Ref. [43,44]). Since CLT appears to have variability in the size and number of gaps at the edges, the potential for gravity fed leaks that percolate into the interior of the panel are substantial, particularly with upright wall panels. In these cases, it would be a good precaution to entirely cover the edges during construction. It is advisable to (1) install the panels so that they can passively shed surface water during construction, and (2) avoid moisture trapping by maximizing the amount of air space between element edges (particularly between two porous elements). Detailing should consider avoiding moisture trapping conditions for both in service and construction conditions.

Since moisture would appear to accumulate at the upper one or two plies during exposure to rain, covering of CLT floor panels with a concrete screed or impermeably membrane after exposure will likely retard drying rates [21]. On the other hand, there may be a benefit to applying a screed prior to exposure to reduce wetting of CLT floor panels. With these considerations in mind, it seems it would be prudent to (1) delay enclosure of an assembly until all layers were below a designated threshold MC (ideally less than 16% [9], and/or (2) to build the floor assembly offsite, in dry and controlled conditions. The latter would be particularly advantageous, especially coupled with envelope prefabrication, since it would reduce on-site construction time. In the case of pouring/assembling on site, one month of drying after exposure might be an economical minimum, since the majority of drying was observed to occur within the first month, and occurred primarily at the

upper surfaces where drying would be most inhibited by impermeable assembly components.

Rapid drying of CLT for enclosure within assemblies should be controlled, as it will likely result in checking and distortions if done too rapidly. Since surfaces will dry faster than the core, it is advisable to monitor also the interior MC (e.g., plies 2 and 3), and particularly at vulnerable locations (e.g., connections). Since the edges of CLT are the most likely to swell and contract, it is important to take into consideration the effects this might have on hardware and connections during the construction process. Finally, connection design should assume higher levels of deterioration at the edges of panels as a result of cyclic weathering.

Acknowledgements

Thank you, Milo Clauson, Frederik Laleicke, and Ariel Muldoon for your assistance during this study.

The "SMART-CLT" project is conducted through the TallWood Design Institute with funding by the U.S. Department of Agriculture's Agricultural Research Service (Agreement No. 58-0202-5-001). The material presented in this contribution is also based upon work that is supported by the National Institute of Food and Agriculture, USDA McIntire Stennis project under 1009740.

Appendix. Discontinuous moisture measurements

Table 3

Discontinuous moisture measurements at the front locations of the sample. Bold/red values highlight MC above 16% (standard dry service conditions [9]), while underlined values highlight the highest MC for a given ply. Shaded regions are measurements taken after a period drying (prior to wetting).

	Depth (cm)	BEFORE wetting 1 **duration -45 days**			AFTER wetting 1 **duration 12 days**			AFTER wetting 2 **duration 97 days**			BEFORE wetting 3 **duration 144 days**			AFTER wetting 3 **duration 147 days**		
		F1a	--	F3a*	F1	F2	F3	F1	F2	F3	F1	F2	F3	F1	F2**	F3
PLY 1	1.3	--	--	--	--	--	--	**18.2**	12.3	--	8.7	9.0	10.5	**16.4**	10.0	15.6
	1.9	11.0	--	10.7	**19.5**	**18.2**	**16.5**	**22.0**	**17.1**	**17.5**	9.7	9.9	11.0	15.3	10.9	15.8
	2.5	--	--	--	--	--	--	**25.6**	**19.8**	**21.1**	10.1	10.8	11.7	12.2	11.9	15.5
	3.2	--	--	--	--	--	--	**30.8**	**26.6**	**21.6**	10.6	11.7	12.1	13.9	14.8	**17.6**
PLY 2	3.8	--	--	--	--	--	--	--	--	--	9.5	12.3	12.9	**16.5**	**20.7**	**20.0**
	4.4	--	--	--	--	--	--	**18.6**	**19.5**	**27.9**	10.6	12.2	12.9	15.3	15.5	12.4
	5.1	14.3	--	13.4	**16.5**	**16.9**	**28.7**	**17.7**	**15.3**	**26.3**	11.8	12.3	13.4	14.7	13.6	13.1
	5.7	--	--	--	--	--	--	**16.2**	12.5	**24.8**	12.1	12.2	14.1	13.3	13.1	14.1
	6.4	--	--	--	--	--	--	15.8	--	--	12.3	12.3	14.1	12.7	13.9	15.1
PLY 3	7.6	--	--	--	--	--	--	13.1	11.9	14.7	11.7	13.5	14.9	13.1	**16.2**	15.8
	8.1	**16.3**	--	13.5	15.3	**16.2**	**16.6**	14.7	12.8	**16.8**	11.7	13.4	14.5	12.2	12.4	14.3

*: an asterisk denotes that values in a column are averages of two measurements. A double asterisk denotes that values in a column are averages of three measurements.

Table 4

Discontinuous moisture measurements near the half lap joint. Bold/red values highlight MC above 16% (standard dry service conditions [9]), while underlined values highlight the highest MC for a given ply. Shaded regions are measurements taken after a period drying (prior to wetting).

	Depth (cm)	BEFORE wetting 1 **duration -45 days**		AFTER wetting 1 **duration 12 days**		AFTER wetting 2 **duration 97 days**		BEFORE wetting 3 **duration 144 days**		AFTER wetting 3 **duration 147 days**	
		M1a	M2	M1	M2	M1	M2	M1	M2	M1	M2
PLY 1	1.3	--	--	--	--	14.1	12.3	12.2	11.4	11.8	11.6
	1.9	10.1	--	14.0	14.3	15.6	13.9	13.6	12.3	13.0	11.2
	2.5	--	--	--	--	**17.1**	14.7	14.3	13.0	14.6	12.8
	3.2	--	--	--	--	**25.0**	**16.0**	**14.5**	**13.8**	**21.6**	**13.0**
PLY 2	3.8	--	--	--	--	--	--	**16.0**	**16.5**	**17.4**	13.6
	4.4	--	--	--	--	**19.5**	**18.5**	**16.6**	**18.2**	**17.7**	15.0
	5.1	13.9	--	15.4	15.5	**20.2**	**19.5**	**17.3**	**19.4**	**18.7**	**16.3**
	5.7	--	--	--	--	**19.8**	**20.2**	**17.5**	**19.9**	**18.6**	**17.2**
	6.4	--	--	--	--	--	--	**17.2**	**19.5**	**18.7**	**17.6**
PLY 3	7.6	--	--	--	--	**18.2**	**27.8**	**16.5**	**18.0**	**18.2**	**21.5**
	8.1	14.3	--	14.6	**20.7**	**18.2**	**26.2**	**17.3**	**18.9**	**18.2**	**17.7**

Table 5

Discontinuous moisture measurements at the sheltered rear portion of the panel. Bold/red values highlight MC above 16% (standard dry service conditions [9]), while underlined values highlight the highest MC for a given ply. Shaded regions are measurements taken after a period drying (prior to wetting).

	Depth (cm)	BEFORE wetting 1 **duration -45 days**			AFTER wetting 1 **duration 12 days**			AFTER wetting 2 **duration 97 days**			BEFORE wetting 3 **duration 144 days**			AFTER wetting 3 **duration 147 days**		
		R1a	--	R3a	R1	R2	R3	R1	R2	R3	R1	R2	R3	R1	R2*	R3
PLY 1	1.3	--	--	--	--	--	--	11.9	12.4	11.4	9.8	10.0	9.6	9.2	14.5	9.4
	1.9	12.0	--	11.4	14.5	14.9	**20.8**	11.8	11.7	11.0	11.4	11.0	10.8	9.4	12.7	9.7
	2.5	--	--	--	--	--	--	12.3	11.9	12.0	11.9	11.7	11.0	10.8	10.3	10.8
	3.2	--	--	--	--	--	--	13.0	12.2	12.9	12.2	11.8	12.0	11.4	11.3	13.4
PLY 2	3.8	--	--	--	--	--	--	--	--	--	12.1	12.8	11.6	11.4	12.1	**19.4**
	4.4	--	--	--	--	--	--	13.3	15.3	14.9	12.2	14.0	11.6	11.2	12.0	14.7
	5.1	**16.0**	--	12.7	13.9	15.2	12.9	12.7	15.0	14.1	12.3	14.4	12.7	11.1	12.5	12.9
	5.7	--	--	--	--	--	--	12.4	15.6	13.2	12.8	14.7	13.0	11.8	12.9	12.5
	6.4	--	--	--	--	--	--	12.5	15.3	12.9	13	14.2	13.4	12.2	12.8	12.9
PLY 3	7.6	--	--	--	--	--	--	13.5	13.1	12.4	12.9	12.9	12.1	12.8	12.4	12.0
	8.1	13.2	--	11.7	14.1	13.8	13.9	13.8	13.4	12.5	13.3	13.1	12.7	13.3	12.8	12.7

*: An asterisk in this table denotes that values in a column are averages of two measurements.

References

[1] R.H. Crawford, X. Cadorel, A framework for assessing the environmental benefits of mass timber construction, Proc. Eng. 196 (June) (2017) 838–846.

[2] Gamper, P. Dietsch, M. Merk, S. Winter, Building Climate - long-term measurements to determine the effect on the moisture gradient in large-span timber structures | Gebudeklima - Langzeitmessung zur Bestimmung der Auswirkungen auf Feuchtegradienten in Holzbauteilen, Bautechnik 90 (8) (2013).

[3] S.V. Glass, S.L. Zelinka, Chapter 4 - moisture relations and physical properties of wood, Wood Handbook - Wood as an Engineering Material, 2010, pp. 1–20.

[4] R. Shmulsky, P.D. Jones, Forest Products and Wood Science an Introduction, sixth ed., (2011).

[5] J. Wang, E. Karsh, G. Finch, M. Chen, Field measurement of vertical movement and roof moisture performance of the wood innovation and design centre, Proc. WCTE 2016 World Conf. Timber Eng. Vienna/Austria, 2016, pp. 2–3. August 22-25, 2016, no. Lvl.

[6] G. Mustapha, K. Khondoker, J. Higgins, Moisture performance and vertical movement monitoring of pre-fabricated cross laminate timber – featured case Study : Ubc Tallwood House, 15th Canadian Conference on Building Science and Technology, 2017, pp. 1–15.

[7] P. Dietsch, A. Brunauer, Reinforcement of timber structures – a new section for EC 5, Proc. International Conference on Connections in Timber Engineering – from Research to Standards, Graz, Austria, 2017, pp. 184–211.

[8] American Wood Council, National Design Specification (NDS) for Wood Construction 2018 Edition, American Wood Council, 2018.

[9] American National Standard, Standard for Performance-rated Cross-laminated timber. (ANSI/APA PRG 320-2017), APA, 2017.

[10] J. Koch, A. Simon, R.W. Arndt, Monitoring of moisture content of protected timber bridges, Proc. WCTE 2016 World Conf. Timber Eng. Vienna/Austria, 2016 August 22-25.

[11] A. Gülzow, K. Richter, R. Steiger, Influence of wood moisture content on bending and shear stiffness of cross laminated timber panels, Eur. J. Wood Wood Prod. 69 (2) (2011) 193–197.

[12] C. Silva, J.M. Branco, A. Ringhofer, P.B. Lourenço, G. Schickhofer, The influences of moisture content variation, number and width of gaps on the withdrawal resistance of self tapping screws inserted in cross laminated timber, Construct. Build. Mater. 125 (2016) 1205–1215, https://doi.org/10.1016/j.conbuildmat.2016.09.008.

[13] C.C. Gerhards, Effect of moisture content and temperature on the mechanical properties of wood: an analysis of immediate effects, Wood Fiber Sci. 14 (1982) 4–36, https://doi.org/10.1079/PHN2004659.

[14] D.W. Green, J.W. Evans, Evolution of Standardized Procedures for Adjusting Lumber Properties for Change in Moisture Content. General Technical Report FPL – GTR – 127, U.S. Department of Agriculture, Forest Service, Forest Products Laboratory, Madison, WI, U.S., 2001.

[15] R.T.M. Lepage, Moisture Response of Wall Assemblies of Cross- Laminated Timber Construction in Cold Canadian Climates, Thesis Civ. Eng. Universiy Waterloo, Ontario, Canada, 2012, p. 139.

[16] G. Alsayegh, P. Mukhopadhyaya, J. Wang, E. Zalok, D. van Reenen, Preliminary characterization of physical properties of cross-laminated-timber (CLT) panels for hygrothermal modelling, Adv. Civ. Eng. Mater. 2 (1) (2013) 20120048.

[17] J. Tripathi, Hygrothermal Properties of Cross Laminated Timber Panels, Thesis University of Maine, 2012.

[18] R. Popper, P. Niemz, G. Eberle, Equilibrium moisture content and swelling of the solid wood panels, Holz Als Roh-Und Werkst. 62 (3) (2004) 209–217.

[19] R. McClung, H. Ge, J. Straube, J. Wang, Hygrothermal performance of cross-laminated timber wall assemblies with built-in moisture: field measurements and simulations, Build. Environ. 71 (January) (2014) 95–110.

[20] J. Wang, Wetting and drying performance of wood-based assemblies related to on-site moisture management, Proc. WCTE 2016 World Conf. Timber Eng. Vienna/Austria, 2016, pp. 1–22 no. 2, August 22-25.

[21] J.H. Robert Lepage, Graham Finch, Moisture uptake testing for CLT floor panels in a tall wood building in Vancouver, 15th Canadian Conference on Building Science and Technology, 2017, pp. 1–17 no. Mc.

[22] S. Kordziel, Study of Moisture Conditions in a Multi-storey Mass Timber Building through the Use of Sensors and WUFI Hygrothermal Modeling, M.S. Thesis Colorado School of Mines, 2017.

[23] E. Schmidt, M. Riggio, A. Barbosa, P.F. Laleicke, K. van den Wymelenberg, How monitoring CLT buildings can remove market barriers and support designers in North America: an introduction to preliminary environmental studies, Rev. Port. Eng. Estruturas (Portuguese J. Struct. Eng.) 7 (III) (July 2018) 41–48.

[24] E. Schmidt, M. Riggio, A. Barbosa, I. Mugabo, P.F. Laleicke, Moisture response of a full-scale cross laminated timber panel during environmental simulation: key factors in design and management, World Conference of Timber Engineering, August 20-23, 2018 Seoul, Rep. of Korea.

[25] J. Niklewski, T. Isaksson, E. Frühwald Hansson, S. Thelandersson, Moisture conditions of rain-exposed glue-laminated timber members: the effect of different detailing, Wood Mater. Sci. Eng. 0272 (2017) 1–12.

[26] USA gov, National Weather Service Forecast Office: Portland, Oregon. [Online]. Available: http://www.wrh.noaa.gov/pqr/pdxclimate/pg6.pdf; https://www.wrh.noaa.gov/pqr/pdxclimate/pg125.pdf; http://w2.weather.gov/climate/local_data.php?wfo=pqr. [Accessed: 08-Jun-2017].

[27] E. Schmidt, Moisture Monitoring of Cross Laminated Timber Building Components, M.S. Thesis Oregon State University, 2018.

[28] P. Dietsch, S. Franke, B. Franke, A. Gamper, S. Winter, Methods to determine wood moisture content and their applicability in monitoring concepts, J. Civ. Struct. Heal. Monit. 5 (2) (2014) 115–127.

[29] ASTM International ASTM D4761-13 Standard Test Methods for Mechanical Properties of Lumber and Wood-Base Structural Material, (2013), https://doi.org/10.1520/D4761-13.

[30] V. Mahdavifar, Cyclic performance of connections used in hybrid cross-laminated timber, Available at: https://ir.library.oregonstate.edu/concern/graduate_thesis_or_dissertations/1j92gc89f, (2017) Ph.D. Dissertation.

[31] G. Wengert, P. Bois, Evaluation of electric moisture meters on kiln-dried lumber, For. Prod. J. 47 (6) (June 1997) 60–62.

[32] P. Wilson, Accuracy of a capacitance-type and three resistance-type pin meters for measuring wood moisture content, For. Prod. J. 49 (9) (1999) 29–32 Sep.

[33] K. Sandberg, A. Pousette, Moisture conditions in coated glulam beams and columns during weathering, International Conference on Durability of Building Materials and Components, 2011, pp. 1–8.

[34] N. Björngrim, O. Hagman, X.A. Wang, Moisture content monitoring of a timber footbridge, BioResources 11 (2) (2016) 3904–3913.

[35] L. Jorge, A. Dias, R. Costa, Performance of X-Lam panels in a sports center with an indoor swimming-pool, J. Civ. Struct. Heal. Monit. 5 (2) (2015) 129–139.

[36] S. MuGrauer, Personal Communication, (2017) September 29th.

[37] Franke, S. Franke, M. Schiere, and A. Müller, Moisture diffusion in wood – experimental and numerical investigations, Proc. WCTE 2016 World Conf. Timber Eng. Vienna/Austria, August 22-25, 2016.

[38] J. Morrell, I. Morrell, A. Sinha, D. Trebelhorn, Moisture intrusion in cross laminated timber and the potential for fungal attack, Proc. WCTE 2018 World Conf. Timber Eng. Seoul/S. Korea, 2018 August 20-23.
[39] F. Lanata, Monitoring the long-term behaviour of timber structures, J. Civ. Struct. Heal. Monit. 5 (2) (2015) 167–182.
[40] APA, The Engineered Wood Association, Owner 's Guide to Understanding Checks in Glued Laminated Timber, (2006).
[41] R. Bergman, Chapter 13 - Drying and Control of Moisture Content and Dimensional Changes, Wood Handb. - Wood as an Eng. Mater. (2010), pp. 1–20.
[42] J.A. Nairn, Cross laminated timber properties including effects of non-glued edges and additional cracks, Eur. J. Wood Wood Prod. 75 (6) (2017) 973–983.
[43] E. Serrano, Limnologen – experiences from an 8- storey timber building, Internationales Holzbau-forum 09, 2009, pp. 1–12.
[44] Leyder, F. Wanninger, A. Frangi, E. Chatzi, Dynamic response of an innovative hybrid structure in hardwood, Proc. Inst. Civ. Eng. - Constr. Mater. 168 (3) (2015) 132–143.